EUROPEAN ORGANIZATION FOR NUCLEAR RESEARCH

CERN–EP/2003-044

21 Avril 2003

A measurement of the branching fractions of the b-quark into charged and neutral b-hadrons

DELPHI Collaboration

Abstract

The production fractions of charged and neutral b-hadrons in b-quark events from Z^0 decays have been measured with the DELPHI detector at LEP. An algorithm has been developed, based on a neural network, to estimate the charge of the weakly-decaying b-hadron by distinguishing its decay products from particles produced at the primary vertex. From the data taken in the years 1994 and 1995, the fraction of $\overline{b}$-quarks fragmenting into positively charged weakly-decaying b-hadrons has been measured to be:

$$f^+ = (42.09 \pm 0.82(\text{stat.}) \pm 0.89(\text{syst.}))\%.$$

Subtracting the rates for charged $\overline{\Xi}_b^+$ and $\overline{\Omega}_b^+$ baryons gives the production fraction of B^+ mesons:

$$f_{B_u} = (40.99 \pm 0.82(\text{stat.}) \pm 1.11(\text{syst.}))\%.$$

(Accepted by PLB)

J.Abdallah[25], P.Abreu[22], W.Adam[51], P.Adzic[11], T.Albrecht[17], T.Alderweireld[2], R.Alemany-Fernandez[8], T.Allmendinger[17], P.P.Allport[23], U.Amaldi[29], N.Amapane[45], S.Amato[48], E.Anashkin[36], A.Andreazza[28], S.Andringa[22], N.Anjos[22], P.Antilogus[25], W-D.Apel[17], Y.Arnoud[14], S.Ask[26], B.Asman[44], J.E.Augustin[25], A.Augustinus[8], P.Baillon[8], A.Ballestrero[46], P.Bambade[20], R.Barbier[27], D.Bardin[16], G.Barker[17], A.Baroncelli[39], M.Battaglia[8], M.Baubillier[25], K-H.Becks[53], M.Begalli[6], A.Behrmann[53], E.Ben-Haim[20], N.Benekos[32], A.Benvenuti[5], C.Berat[14], M.Berggren[25], L.Berntzon[44], D.Bertrand[2], M.Besancon[40], N.Besson[40], D.Bloch[9], M.Blom[31], M.Bluj[52], M.Bonesini[29], M.Boonekamp[40], P.S.L.Booth[23], G.Borisov[21], O.Botner[49], B.Bouquet[20], T.J.V.Bowcock[23], I.Boyko[16], M.Bracko[43], R.Brenner[49], E.Brodet[35], P.Bruckman[18], J.M.Brunet[7], L.Bugge[33], P.Buschmann[53], M.Calvi[29], T.Camporesi[8], V.Canale[38], F.Carena[8], N.Castro[22], F.Cavallo[5], M.Chapkin[42], Ph.Charpentier[8], P.Checchia[36], R.Chierici[8], P.Chliapnikov[42], J.Chudoba[8], S.U.Chung[8], K.Cieslik[18], P.Collins[8], R.Contri[13], G.Cosme[20], F.Cossutti[47], M.J.Costa[50], B.Crawley[1], D.Crennell[37], J.Cuevas[34], J.D'Hondt[2], J.Dalmau[44], T.da Silva[48], W.Da Silva[25], G.Della Ricca[47], A.De Angelis[47], W.De Boer[17], C.De Clercq[2], B.De Lotto[47], N.De Maria[45], A.De Min[36], L.de Paula[48], L.Di Ciaccio[38], A.Di Simone[39], K.Doroba[52], J.Drees[53,8], M.Dris[32], G.Eigen[4], T.Ekelof[49], M.Ellert[49], M.Elsing[8], M.C.Espirito Santo[22], G.Fanourakis[11], D.Fassouliotis[11,3], M.Feindt[17], J.Fernandez[41], A.Ferrer[50], F.Ferro[13], U.Flagmeyer[53], H.Foeth[8], E.Fokitis[32], F.Fulda-Quenzer[20], J.Fuster[50], M.Gandelman[48], C.Garcia[50], Ph.Gavillet[8], E.Gazis[32], R.Gokieli[8,52], B.Golob[43], G.Gomez-Ceballos[41], P.Goncalves[22], E.Graziani[39], G.Grosdidier[20], K.Grzelak[52], J.Guy[37], C.Haag[17], A.Hallgren[49], K.Hamacher[53], K.Hamilton[35], S.Haug[33], F.Hauler[17], V.Hedberg[26], M.Hennecke[17], H.Herr[8], J.Hoffman[52], S-O.Holmgren[44], P.J.Holt[8], M.A.Houlden[23], K.Hultqvist[44], J.N.Jackson[23], G.Jarlskog[26], P.Jarry[40], D.Jeans[35], E.K.Johansson[44], P.D.Johansson[44], P.Jonsson[27], C.Joram[8], L.Jungermann[17], F.Kapusta[25], S.Katsanevas[27], E.Katsoufis[32], G.Kernel[43], B.P.Kersevan[8,43], U.Kerzel[17], A.Kiiskinen[15], B.T.King[23], N.J.Kjaer[8], P.Kluit[31], P.Kokkinias[11], C.Kourkoumelis[3], O.Kouznetsov[16], Z.Krumstein[16], M.Kucharczyk[18], J.Lamsa[1], G.Leder[51], F.Ledroit[14], L.Leinonen[44], R.Leitner[30], J.Lemonne[2], V.Lepeltier[20], T.Lesiak[18], W.Liebig[53], D.Liko[51], A.Lipniacka[44], J.H.Lopes[48], J.M.Lopez[34], D.Loukas[11], P.Lutz[40], L.Lyons[35], J.MacNaughton[51], A.Malek[53], S.Maltezos[32], F.Mandl[51], J.Marco[41], R.Marco[41], B.Marechal[48], M.Margoni[36], J-C.Marin[8], C.Mariotti[8], A.Markou[11], C.Martinez-Rivero[41], J.Masik[12], N.Mastroyiannopoulos[11], F.Matorras[41], C.Matteuzzi[29], F.Mazzucato[36], M.Mazzucato[36], R.Mc Nulty[23], C.Meroni[28], W.T.Meyer[1], E.Migliore[45], W.Mitaroff[51], U.Mjoernmark[26], T.Moa[44], M.Moch[17], K.Moenig[8,10], R.Monge[13], J.Montenegro[31], D.Moraes[48], S.Moreno[22], P.Morettini[13], U.Mueller[53], K.Muenich[53], M.Mulders[31], L.Mundim[6], W.Murray[37], B.Muryn[19], G.Myatt[35], T.Myklebust[33], M.Nassiakou[11], F.Navarria[5], K.Nawrocki[52], R.Nicolaidou[40], M.Nikolenko[16,9], A.Oblakowska-Mucha[19], V.Obraztsov[42], A.Olshevski[16], A.Onofre[22], R.Orava[15], K.Osterberg[15], A.Ouraou[40], A.Oyanguren[50], M.Paganoni[29], S.Paiano[5], J.P.Palacios[23], H.Palka[18], Th.D.Papadopoulou[32], L.Pape[8], C.Parkes[24], F.Parodi[13], U.Parzefall[8], A.Passeri[39], O.Passon[53], L.Peralta[22], V.Perepelitsa[50], A.Perrotta[5], A.Petrolini[13], J.Piedra[41], L.Pieri[39], F.Pierre[40], M.Pimenta[22], E.Piotto[8], T.Podobnik[43], V.Poireau[8], M.E.Pol[6], G.Polok[18], P.Poropat[†47], V.Pozdniakov[16], N.Pukhaeva[2,16], A.Pullia[29], J.Rames[12], L.Ramler[17], A.Read[33], P.Rebecchi[8], J.Rehn[17], D.Reid[31], R.Reinhardt[53], P.Renton[35], F.Richard[20], J.Ridky[12], M.Rivero[41], D.Rodriguez[41], A.Romero[45], P.Ronchese[36], E.Rosenberg[1], P.Roudeau[20], T.Rovelli[5], V.Ruhlmann-Kleider[40], D.Ryabtchikov[42], A.Sadovsky[16], L.Salmi[15], J.Salt[50], A.Savoy-Navarro[25], U.Schwickerath[8], A.Segar[35], R.Sekulin[37], M.Siebel[53], A.Sisakian[16], G.Smadja[27], O.Smirnova[26], A.Sokolov[42], A.Sopczak[21], R.Sosnowski[52], T.Spassov[8], M.Stanitzki[17], A.Stocchi[20], J.Strauss[51], B.Stugu[4], M.Szczekowski[52], M.Szeptycka[52], T.Szumlak[19], T.Tabarelli[29], A.C.Taffard[23], F.Tegenfeldt[49], J.Timmermans[31], L.Tkatchev[16], M.Tobin[23], S.Todorovova[12], B.Tome[22], A.Tonazzo[29], P.Tortosa[50], P.Travnicek[12], D.Treille[8], G.Tristram[7], M.Trochimczuk[52], C.Troncon[28], M-L.Turluer[40], I.A.Tyapkin[16], P.Tyapkin[16], S.Tzamarias[11], V.Uvarov[42], G.Valenti[5], P.Van Dam[31], J.Van Eldik[8], A.Van Lysebetten[2], N.van Remortel[2], I.Van Vulpen[8], G.Vegni[28], F.Veloso[22], W.Venus[37], P.Verdier[27], V.Verzi[38], D.Vilanova[40], L.Vitale[47], V.Vrba[12], H.Wahlen[53], A.J.Washbrook[23], C.Weiser[17], D.Wicke[8],

J.Wickens[2], G.Wilkinson[35], M.Winter[9], M.Witek[18], O.Yushchenko[42], A.Zalewska[18], P.Zalewski[52], D.Zavrtanik[43], V.Zhuravlov[16], N.I.Zimin[16], A.Zintchenko[16], M.Zupan[11]

[1]Department of Physics and Astronomy, Iowa State University, Ames IA 50011-3160, USA
[2]Physics Department, Universiteit Antwerpen, Universiteitsplein 1, B-2610 Antwerpen, Belgium
and IIHE, ULB-VUB, Pleinlaan 2, B-1050 Brussels, Belgium
and Faculté des Sciences, Univ. de l'Etat Mons, Av. Maistriau 19, B-7000 Mons, Belgium
[3]Physics Laboratory, University of Athens, Solonos Str. 104, GR-10680 Athens, Greece
[4]Department of Physics, University of Bergen, Allégaten 55, NO-5007 Bergen, Norway
[5]Dipartimento di Fisica, Università di Bologna and INFN, Via Irnerio 46, IT-40126 Bologna, Italy
[6]Centro Brasileiro de Pesquisas Físicas, rua Xavier Sigaud 150, BR-22290 Rio de Janeiro, Brazil
and Depto. de Física, Pont. Univ. Católica, C.P. 38071 BR-22453 Rio de Janeiro, Brazil
and Inst. de Física, Univ. Estadual do Rio de Janeiro, rua São Francisco Xavier 524, Rio de Janeiro, Brazil
[7]Collège de France, Lab. de Physique Corpusculaire, IN2P3-CNRS, FR-75231 Paris Cedex 05, France
[8]CERN, CH-1211 Geneva 23, Switzerland
[9]Institut de Recherches Subatomiques, IN2P3 - CNRS/ULP - BP20, FR-67037 Strasbourg Cedex, France
[10]Now at DESY-Zeuthen, Platanenallee 6, D-15735 Zeuthen, Germany
[11]Institute of Nuclear Physics, N.C.S.R. Demokritos, P.O. Box 60228, GR-15310 Athens, Greece
[12]FZU, Inst. of Phys. of the C.A.S. High Energy Physics Division, Na Slovance 2, CZ-180 40, Praha 8, Czech Republic
[13]Dipartimento di Fisica, Università di Genova and INFN, Via Dodecaneso 33, IT-16146 Genova, Italy
[14]Institut des Sciences Nucléaires, IN2P3-CNRS, Université de Grenoble 1, FR-38026 Grenoble Cedex, France
[15]Helsinki Institute of Physics, P.O. Box 64, FIN-00014 University of Helsinki, Finland
[16]Joint Institute for Nuclear Research, Dubna, Head Post Office, P.O. Box 79, RU-101 000 Moscow, Russian Federation
[17]Institut für Experimentelle Kernphysik, Universität Karlsruhe, Postfach 6980, DE-76128 Karlsruhe, Germany
[18]Institute of Nuclear Physics,Ul. Kawiory 26a, PL-30055 Krakow, Poland
[19]Faculty of Physics and Nuclear Techniques, University of Mining and Metallurgy, PL-30055 Krakow, Poland
[20]Université de Paris-Sud, Lab. de l'Accélérateur Linéaire, IN2P3-CNRS, Bât. 200, FR-91405 Orsay Cedex, France
[21]School of Physics and Chemistry, University of Lancaster, Lancaster LA1 4YB, UK
[22]LIP, IST, FCUL - Av. Elias Garcia, 14-1^{o}, PT-1000 Lisboa Codex, Portugal
[23]Department of Physics, University of Liverpool, P.O. Box 147, Liverpool L69 3BX, UK
[24]Dept. of Physics and Astronomy, Kelvin Building, University of Glasgow, Glasgow G12 8QQ
[25]LPNHE, IN2P3-CNRS, Univ. Paris VI et VII, Tour 33 (RdC), 4 place Jussieu, FR-75252 Paris Cedex 05, France
[26]Department of Physics, University of Lund, Sölvegatan 14, SE-223 63 Lund, Sweden
[27]Université Claude Bernard de Lyon, IPNL, IN2P3-CNRS, FR-69622 Villeurbanne Cedex, France
[28]Dipartimento di Fisica, Università di Milano and INFN-MILANO, Via Celoria 16, IT-20133 Milan, Italy
[29]Dipartimento di Fisica, Univ. di Milano-Bicocca and INFN-MILANO, Piazza della Scienza 2, IT-20126 Milan, Italy
[30]IPNP of MFF, Charles Univ., Areal MFF, V Holesovickach 2, CZ-180 00, Praha 8, Czech Republic
[31]NIKHEF, Postbus 41882, NL-1009 DB Amsterdam, The Netherlands
[32]National Technical University, Physics Department, Zografou Campus, GR-15773 Athens, Greece
[33]Physics Department, University of Oslo, Blindern, NO-0316 Oslo, Norway
[34]Dpto. Fisica, Univ. Oviedo, Avda. Calvo Sotelo s/n, ES-33007 Oviedo, Spain
[35]Department of Physics, University of Oxford, Keble Road, Oxford OX1 3RH, UK
[36]Dipartimento di Fisica, Università di Padova and INFN, Via Marzolo 8, IT-35131 Padua, Italy
[37]Rutherford Appleton Laboratory, Chilton, Didcot OX11 OQX, UK
[38]Dipartimento di Fisica, Università di Roma II and INFN, Tor Vergata, IT-00173 Rome, Italy
[39]Dipartimento di Fisica, Università di Roma III and INFN, Via della Vasca Navale 84, IT-00146 Rome, Italy
[40]DAPNIA/Service de Physique des Particules, CEA-Saclay, FR-91191 Gif-sur-Yvette Cedex, France
[41]Instituto de Fisica de Cantabria (CSIC-UC), Avda. los Castros s/n, ES-39006 Santander, Spain
[42]Inst. for High Energy Physics, Serpukov P.O. Box 35, Protvino, (Moscow Region), Russian Federation
[43]J. Stefan Institute, Jamova 39, SI-1000 Ljubljana, Slovenia and Laboratory for Astroparticle Physics,
Nova Gorica Polytechnic, Kostanjeviska 16a, SI-5000 Nova Gorica, Slovenia,
and Department of Physics, University of Ljubljana, SI-1000 Ljubljana, Slovenia
[44]Fysikum, Stockholm University, Box 6730, SE-113 85 Stockholm, Sweden
[45]Dipartimento di Fisica Sperimentale, Università di Torino and INFN, Via P. Giuria 1, IT-10125 Turin, Italy
[46]INFN,Sezione di Torino, and Dipartimento di Fisica Teorica, Università di Torino, Via P. Giuria 1,
IT-10125 Turin, Italy
[47]Dipartimento di Fisica, Università di Trieste and INFN, Via A. Valerio 2, IT-34127 Trieste, Italy
and Istituto di Fisica, Università di Udine, IT-33100 Udine, Italy
[48]Univ. Federal do Rio de Janeiro, C.P. 68528 Cidade Univ., Ilha do Fundão BR-21945-970 Rio de Janeiro, Brazil
[49]Department of Radiation Sciences, University of Uppsala, P.O. Box 535, SE-751 21 Uppsala, Sweden
[50]IFIC, Valencia-CSIC, and D.F.A.M.N., U. de Valencia, Avda. Dr. Moliner 50, ES-46100 Burjassot (Valencia), Spain
[51]Institut für Hochenergiephysik, Österr. Akad. d. Wissensch., Nikolsdorfergasse 18, AT-1050 Vienna, Austria
[52]Inst. Nuclear Studies and University of Warsaw, Ul. Hoza 69, PL-00681 Warsaw, Poland
[53]Fachbereich Physik, University of Wuppertal, Postfach 100 127, DE-42097 Wuppertal, Germany
† deceased

1 Introduction

The branching fractions of the b-quark into the different species of b-hadrons are an important input and source of systematic uncertainty for many measurements in the heavy flavour sector where b-hadrons are produced in jets, e.g. analyses on B-meson oscillations or CKM elements at LEP. Furthermore, these production fractions give insight into the fragmentation process. Since b-quarks at LEP are mainly produced directly in the decay of the Z^0 boson, with negligible contributions from later processes like gluon splitting $g \to b\overline{b}$, b-hadron production fractions are sensitive to a certain step in the fragmentation process, namely the beginning of the fragmentation chain. This is not the case for analyses investigating inclusive particle production rates of hadrons which do not contain a primary heavy quark.

The b-hadron production fractions are defined as the probability of a $\overline{b}$- or b-quark to fragment into the corresponding b-hadron: $f_{B_u} = BR(\overline{b} \to B^+) = BR(b \to B^-)$, $f_{B_d} = BR(\overline{b} \to B^0) = BR(b \to \overline{B}^0)$, $f_{B_s} = BR(\overline{b} \to B_s^0) = BR(b \to \overline{B}_s^0)$, $f_{b-baryon} = BR(\overline{b} \to \text{anti–}b\text{-baryon}) = BR(b \to b\text{-baryon})$. Furthermore, the production fractions for charged and neutral b-hadrons are defined as $f^+ = BR(\overline{b} \to X_B^+) = BR(b \to X_B^-)$ and $f^0 = BR(\overline{b} \to X_B^0) = BR(b \to X_B^0)$, where X_B^+, X_B^- and X_B^0 stand for any positively charged, negatively charged or neutral b-hadron, respectively. With these definitions, f_{B_i} is also the production fraction of the b-hadron type B_i, particle or antiparticle, in $b\overline{b}$-events.

A direct measurement of these production fractions using exclusive decays is difficult, since there are many decay channels with small branching fractions having large relative uncertainties [1]. For the determination of f_{B_s}, the inputs used are measurements of the product branching ratio $BR(\overline{b} \to B_s^0) \cdot BR(B_s^0 \to D_s^- l^+ \nu X)$ at LEP [2], measurements of the ratio $f_{B_s}/(f_{B_u} + f_{B_d})$ using events with exclusively reconstructed charm particles in semileptonic b-decays or double semileptonic decays from CDF [3] and the mixing parameters $\overline{\chi}$ and χ_d. The integrated mixing probability $\overline{\chi}$, in an unbiased sample of neutral B-mesons, has contributions from B^0- and B_s^0-mesons[1]: $\overline{\chi} = f_{B_d}\chi_d + f_{B_s}\chi_s$, where χ_d and χ_s are the integrated mixing probabilities for B^0- and B_s^0-mesons. This allows the extraction of f_{B_s} quite precisely. The baryon rate is estimated from similar product branching ratios, using $\Lambda_c^+ l^-$ and $\Xi^- l^-$ correlations [3,4], and a measurement of proton production in b-hadron decays [5]. No direct measurements of f_{B_d} or f_{B_u} have been published so far. The averages for weakly-decaying b-hadrons are listed in [1]. The following assumptions are made: the b-hadron production fractions are the same in $Z \to b\overline{b}$ decays at LEP and in high-p_t jets at the TEVATRON, $f_{B_s} + f_{b-baryon} + f_{B_u} + f_{B_d} = 1$ and $f_{B_u} = f_{B_d}$. The latter two are applied as constraints in the averaging procedure. The combined result is $f_{B_s} = (10.6 \pm 1.3)\%$, $f_{b-baryon} = (11.8 \pm 2.0)\%$ and $f_{B_d} = f_{B_u} = (38.8 \pm 1.3)\%$.

In Figure 1 a schematic picture of the b-hadron production process is shown. One has to distinguish between the fractions of b-hadrons which are directly produced in the non-perturbative fragmentation process, denoted f_i' in the following, and the fractions of weakly-decaying b-hadrons, f_i. Strong decays of primarily produced b-hadrons can lead to $f_i' \neq f_i$, e.g. the presence of orbitally excited B_s^{**}-mesons with their expected decays $B_s^{**} \to B^{(*)}K$ have the consequence $f_{B_s}' > f_{B_s}$, $f_{B_u}' < f_{B_u}$ and $f_{B_d}' < f_{B_d}$. However, the

[1] Since $\overline{\chi}$ is mainly measured using leptons, the rates f_{B_d} and f_{B_s} have to be weighted by ratios of lifetimes, τ_{B_d}/τ_B and τ_{B_s}/τ_B, respectively. This has been omitted in the formulae for simplicity.

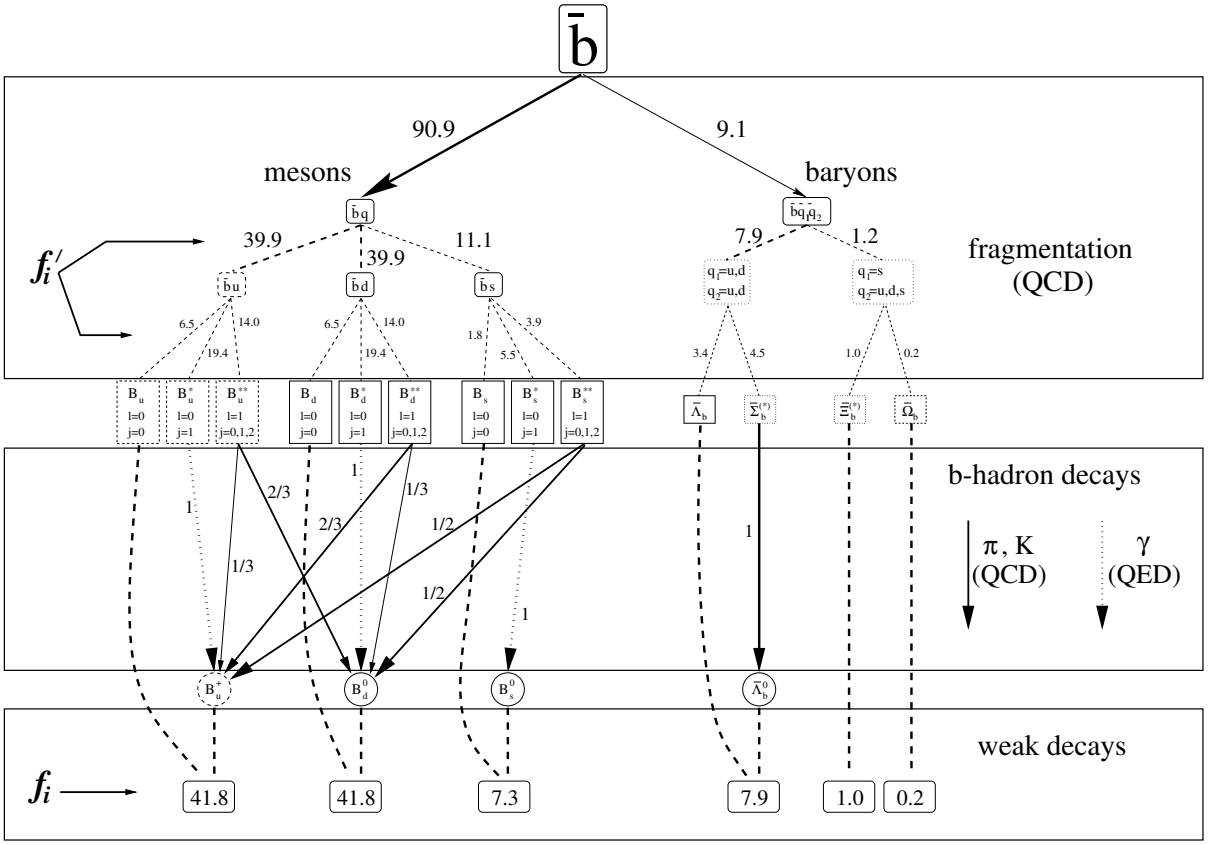

Figure 1: Schematic picture of the production mechanism of b-hadrons. The rates, given in percent, of hadrons primarily produced in the fragmentation are denoted by f', the ones which decay through weak interaction (indicated by dashed lines) by f. Strong and electromagnetic decays are indicated by solid and dotted arrows, respectively, together with their (expected) branching ratios (for strong decays only single pion and kaon transitions have been considered). The given rates are taken from simulation (JETSET 7.3 Monte-Carlo model with parton shower option and parameter settings according to the DELPHI-Tuning [7]). The parameters giving the suppression of $s\overline{s}$ pairs and diquarks are, respectively, $\gamma_s = P(s\overline{s})/P(u\overline{u}) = P(s\overline{s})/P(d\overline{d})$=0.28 and $P(qq)/P(q)$=0.1.

equality $f'_{B_u} = f'_{B_d}$, which originates from isospin symmetry, remains valid for weakly-decaying b-hadrons ($f_{B_u} = f_{B_d}$).[2]

For the rates of charged and neutral b-hadrons, an efficient algorithm has been developed to distinguish charged particles from weak B-decays, from their fragmentation counterparts produced at the primary event vertex. This allows an estimate of the charge of the weakly-decaying hadron to be made and thus a measurement of f^+ and f^0. f_{B_u} can then be extracted from f^+ with small additional uncertainties. The data taken in the years 1994 and 1995, when the DELPHI detector was equipped with a double sided silicon vertex detector, have been used for the analysis.

The simulation used the JETSET 7.3 model [6] with parton shower option and parameters determined from earlier QCD studies [7], followed by a detailed detector simulation [8].

[2]In contrast to the D-system, the presence of B^*-mesons does not change the rates of charged and neutral B-mesons, because their dominant decay mode is $B^* \to B\gamma$. This is also the case for orbitally excited B^{**}-mesons, if $f_{B^{**}_d} = f_{B^{**}_u}$, and isospin rules are used to calculate the dominant single pion transitions.

2 The DELPHI detector and event selection

The DELPHI detector is described in detail in references [9,10]. The present analysis relies mainly on charged particles, measured using information provided by the central tracking detectors.

- The **microVertex Detector** (VD) consists of three layers of silicon strip detectors at radii of 6.3, 9.0 and 10.9 cm. $R\phi$ coordinates[3] in the plane perpendicular to the beam are measured in all three layers. The first and third layers also provide z information. The polar angle (θ) coverage for a particle passing all three layers is from 44° to 136°. The single point precision has been estimated from real data to be about 8 μm in $R\phi$ and (for charged particles crossing perpendicular to the module) about 9 μm in z.
- The **Inner Detector** (ID) consists of an inner drift chamber with jet chamber geometry and 5 cylindrical layers of multiwire proportional chambers (MWPC). The jet chamber, between 12 and 23 cm in R and 23° and 157° in θ, consists of 24 azimuthal sectors, each providing up to 24 $R\phi$ points. From 1995 on, a longer ID has been operational, with polar angle coverage from 15° to 165° and replacing the MWPC by 5 layers of straw tube detectors. The precision on local track elements has been measured in muon pair events to be about 45 μm in $R\phi$.
- The **Time Projection Chamber** (TPC) is the main tracking device of DELPHI. It provides up to 16 space points per particle trajectory for radii between 40 and 110 cm and polar angles between 39° and 141°. The precision on the track elements is about 150 μm in $R\phi$ and about 600 μm in z. For particle identification a measurement of the specific energy loss (dE/dx) is provided by 192 sense wires located at the end caps of the drift volume.
- The **Outer Detector** (OD) consists of 5 layers of drift tubes between radii of 197 and 206 cm. Its polar angle coverage is from 42° to 138°. The OD provides 3 space points and 2 $R\phi$ points per track. The single point precision is about 110 μm in the $R\phi$ plane and about 3.5 cm in the z direction.

An event has been selected as multihadronic if the following requirements are satisfied:

- There must be at least 5 charged particles in the event, each with momentum larger than 400 MeV/c and polar angle between 20° and 160°.
- The total reconstructed energy of these charged particles has to exceed 12% of the centre-of-mass energy (assuming all particles to have the pion mass).
- The total energy of the charged particles in each hemisphere (defined by the plane perpendicular to the beam axis) has to exceed 3% of the centre-of-mass energy.

After these cuts, about 2 million events from the 1994 and 1995 runs have been retained. About 7 million simulated $Z^0 \to q\overline{q}$ and 3.1 million $Z^0 \to b\overline{b}$ events have been selected with the same cuts.

Jets have been reconstructed with the LUCLUS algorithm [6] ($d_{join} = 5$ GeV/c) using charged and neutral particles. Two-jet events well within the acceptance of the vertex detector ($|\cos\theta_{thrust}| < 0.65$) were selected. The event was divided in two hemispheres by the plane perpendicular to the thrust axis.

The most important variables to tag or antitag $b\overline{b}$ events are the track impact parameters of charged particles with respect to the primary vertex which is fit on an event-by-event basis using the position and size of the beamspot as constraints. From the track

[3] In the standard DELPHI coordinate system, the z axis is along the electron direction, the x axis points towards the centre of LEP, and the y axis points upwards. The polar angle to the z axis is denoted by θ, and the azimuthal angle around the z axis by ϕ; the radial coordinate is $R = \sqrt{x^2 + y^2}$.

impact parameters and their errors a probability is computed that a selected sample of charged particles originates from the primary vertex. To increase efficiency and purity, additional information e.g. from reconstructed secondary vertices and identified leptons are used. A combined discriminating variable is then used to select $b\overline{b}$ events. These methods are described in detail in [11]. The tagging of $b\overline{b}$ events was performed in the hemisphere opposite to the one which was used for the measurement. The cut on the discriminating variable of the combined b-tagging has been chosen to give a b-purity of about 97.5%. A secondary vertex was fit in the hemisphere considered for the measurement. Hadronic interactions in the detector material were reconstructed using the algorithm described in [12]. Since the particle causing the interaction is lost in most of the cases, hemispheres with such interactions were rejected.

3 Measurement of the rates of charged and neutral b-hadrons

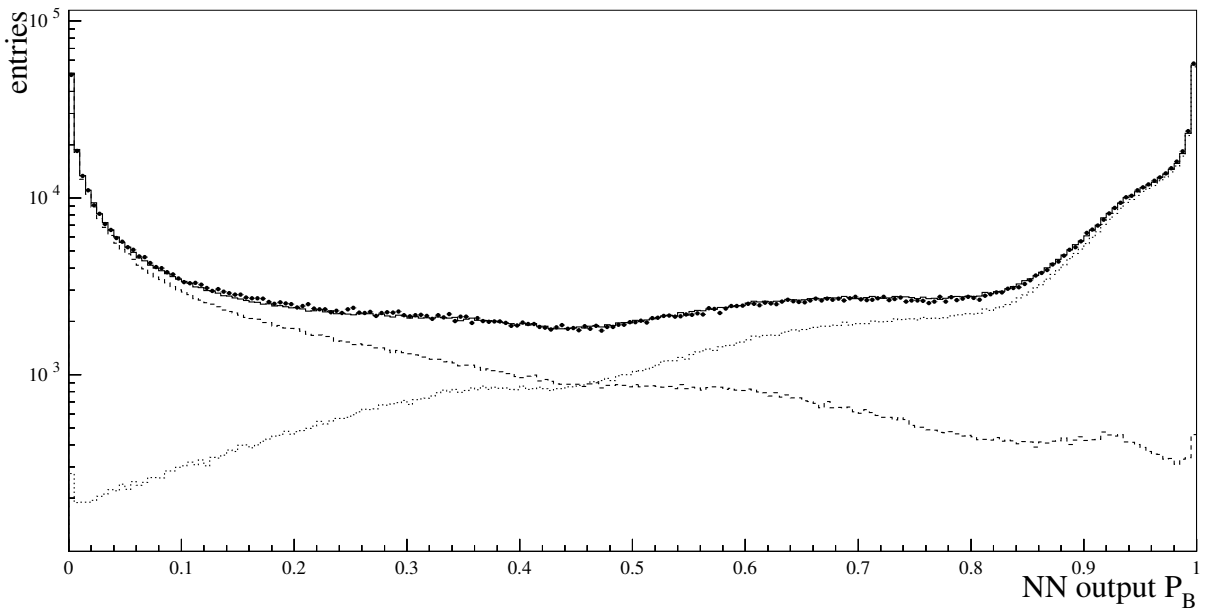

Figure 2: The output of the neural network used to separate B-decay particles from fragmentation particles. Shown are the data (closed circles), the simulation (solid histogram) and the contributions from weak B-decay particles (dotted) and their fragmentation counterparts produced at the primary vertex (dashed). The latter distribution includes particles originating from strong decays of excited b-hadrons.

The basic idea for measuring the rates of charged and neutral b-hadrons is to reconstruct the charge of the weakly-decaying hadron. Based on a neural network, for each charged particle in a hemisphere, a probability P_B that the particle originates from a b-hadron decay rather than from fragmentation is calculated. Charged particles are accepted if their momentum exceeds 500 MeV/c and if at least one vertex detector hit has been associated. At least four charged particles had to be accepted in the hemisphere. The maximum number of charged particles in the hemisphere failing these acceptance cuts was limited to four. The input variables to the neural network are the probability that the charged particle track fits to the primary vertex, the momentum, the rapidity

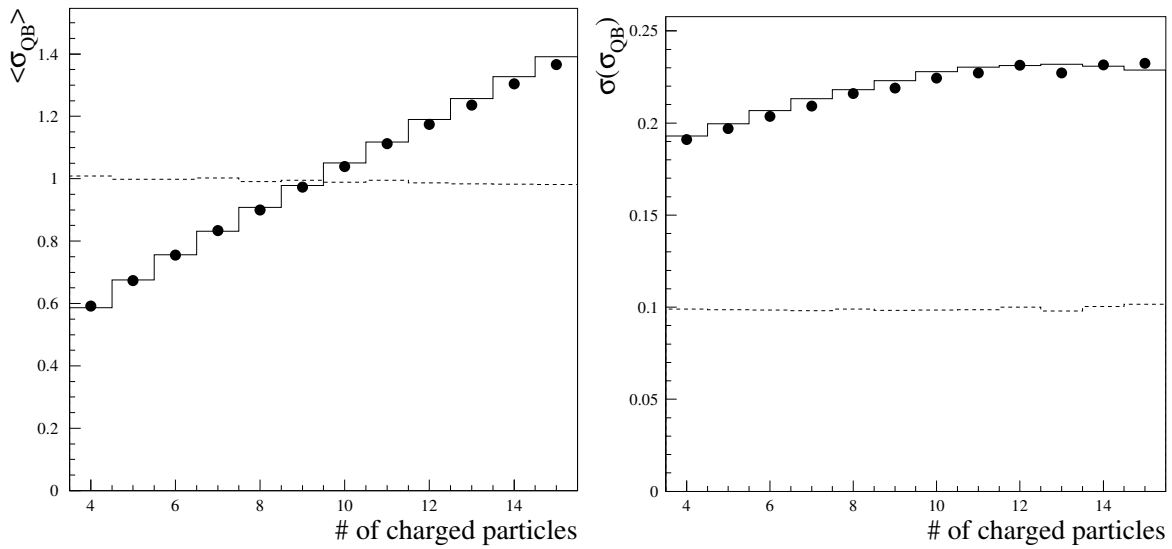

Figure 3: $\langle\sigma_{Q_B}\rangle$ (left) and $\sigma(\sigma_{Q_B})$ (right) versus the number of charged particles which have been used for the estimation of the vertex charge for data (closed circles) and simulation (histogram) before applying the correction as explained in the text. The ratios $\langle\sigma_{Q_B}\rangle_{data}/\langle\sigma_{Q_B}\rangle_{sim.}$ and $0.1\cdot\sigma(\sigma_{Q_B})_{data}/\sigma(\sigma_{Q_B})_{sim.}$ are shown as dashed lines. The deviations are within $\pm 3\%$ over the whole range.

of the particle with respect to the thrust axis, the reconstructed flight distance from the primary to the secondary vertex in the $R\phi$ plane and its error. The last two are not specific for the particles but for the hemisphere considered. They give additional information about the separation power of the other variables, especially the vertex probability. The distributions of the net output variable[4] are shown in Figure 2.[5]

A secondary-vertex charge Q_B is then constructed through

$$Q_B = \sum_{i=1}^{N_{hem}} Q_i P_{B,i} \quad , \tag{1}$$

where N_{hem} is the number of accepted particles in the hemisphere, Q_i the charge of particle i and $P_{B,i}$ its probability to stem from a b-hadron decay as defined above. Assuming binomial statistics, an error on Q_B can be defined as

$$\sigma_{Q_B} = \sqrt{\sum_{i=1}^{N_{hem}} P_{B,i}(1-P_{B,i})} \quad . \tag{2}$$

This quantity does not account for particle losses due to inefficiencies in the track reconstruction. σ_{Q_B} is small if all charged particles are well classified, having values of P_B close to 0 or 1, and gets larger the more particles have probabilities around 0.5.

Parameters in the simulation possibly having an effect on the measurement have been adjusted to their measured values. They are discussed in detail in section 4 and listed also in Table 1.

[4]This variable can be interpreted as Bayesian a-posteriori probability. P_B is computed from this variable taking into account the ratio of b-hadron decay particles and fragmentation particles as taken from simulation. This is necessary because the neural network has been trained with equal numbers of charged particles from these two classes.

[5]If not explicitely stated otherwise, all figures show the data from 1994 and 1995.

The shapes of the Q_B distributions are directly affected by the number of charged particles which have been used in the reconstruction of the vertex charge. This number is larger in the data than in the simulation by 0.12 at a mean value of about 8.0. The shape of the particle multiplicity distribution is very similar in the data and the simulation. The simulated events are reweighted to get agreement in this distribution. The error of the vertex charge, defined in equation 2, also influences the Q_B distributions because it is directly related to its width. Incorrect modelling of the shape of the Q_B distribution in the simulation potentially biases the result. The dependence of the mean value and spread of σ_{Q_B} on the number of charged particles is shown in Figure 3. Data and simulation agree well, the deviations being within $\pm 3\%$. The simulated events are reweighted to get these distributions in agreement, individually for any number of charged particles, to avoid any possible bias. To correct for the loss of charged particle tracks, the number of charged particles in the hemisphere not passing the track cuts is also brought into agreement. All these corrections are small. Comparing the Q_B distributions of data and simulation shows slight shifts of the data distribution with respect to the simulation which is corrected depending on the absolute value of the polar angle θ (these shifts are typically around 0.01 with the deviations from zero not being very significant). Such shifts can be caused by small differences in the material distribution of the detector in data and simulation causing a charge asymmetry.

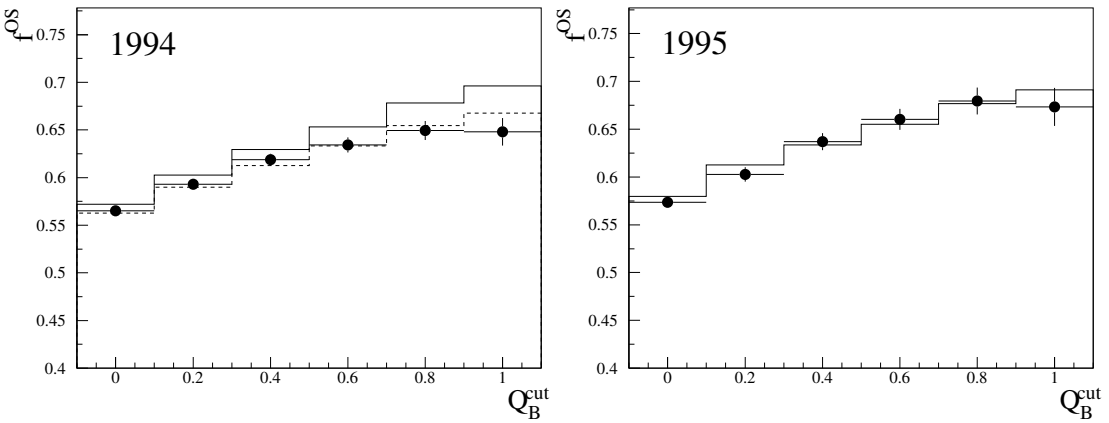

Figure 4: The fraction of 'opposite-sign' events versus Q_B^{cut} for 1994 (left) and 1995 (right) comparing data (circles with error bars) and simulation (histogram), used for the calibration of Q_B. For 1994, the solid (dashed) histogram shows the simulation before (after) applying the correction explained in the text.

The vertex charge Q_B is sensitive to the charge of the b-quark in the hemisphere, mainly in cases where charged b-hadrons are produced. Since b- and $\overline{b}$-quarks are produced in pairs in Z decays, events where the vertex charge Q_B can be determined in both hemispheres ('double tagged' events in the following) can be used to calibrate Q_B on the data themselves. This is done in the following way. For 20116 events, where all cuts are passed in both hemispheres, 'opposite-sign' (called 'OS' in the following) and 'same-sign' ('SS') events are defined through the vertex charges in both hemispheres: OS: $Q_B^1 \cdot Q_B^2 < 0$, SS: $Q_B^1 \cdot Q_B^2 > 0$. To be sensitive to the shape of the distributions, $|Q_B^{1,2}| > Q_B^{cut}$ has been required. The fractions of OS and SS events are directly related to the probability to tag the charge of the b-quark in the hemisphere correctly. In Figure 4, the fraction of OS events, f^{OS}, versus Q_B^{cut} is shown for the 1994 and 1995 data sets. It can

be seen that the probability to tag the b-quark charge correctly is slightly overestimated in the simulation for 1994 (with a tendency to become worse when increasing Q_B^{cut}, thus probing the wings of the distribution), whereas good agreement is found for 1995. The fraction of OS events is mainly determined by the Q_B distributions of charged b-hadrons. To correct for the disagreement between data and simulation in 1994, the Q_B distributions for positively and negatively charged b-hadrons are reweighted in the simulation according to $w^{\pm} = 1 - (\pm a_1 \cdot Q_B - a_2)^3$. The following parameters were found to make the fraction of OS events in the simulation consistent with the data over almost the full range of Q_B^{cut} (see Figure 4): $a_1 = 0.31$ and $a_2 = 0.34$. Another, related, distribution is the fraction of double tagged events versus Q_B^{cut} with respect to all double tagged events. It has been verified that this distribution is in good agreement for both years of data taking (after applying the correction to the 1994 simulation).

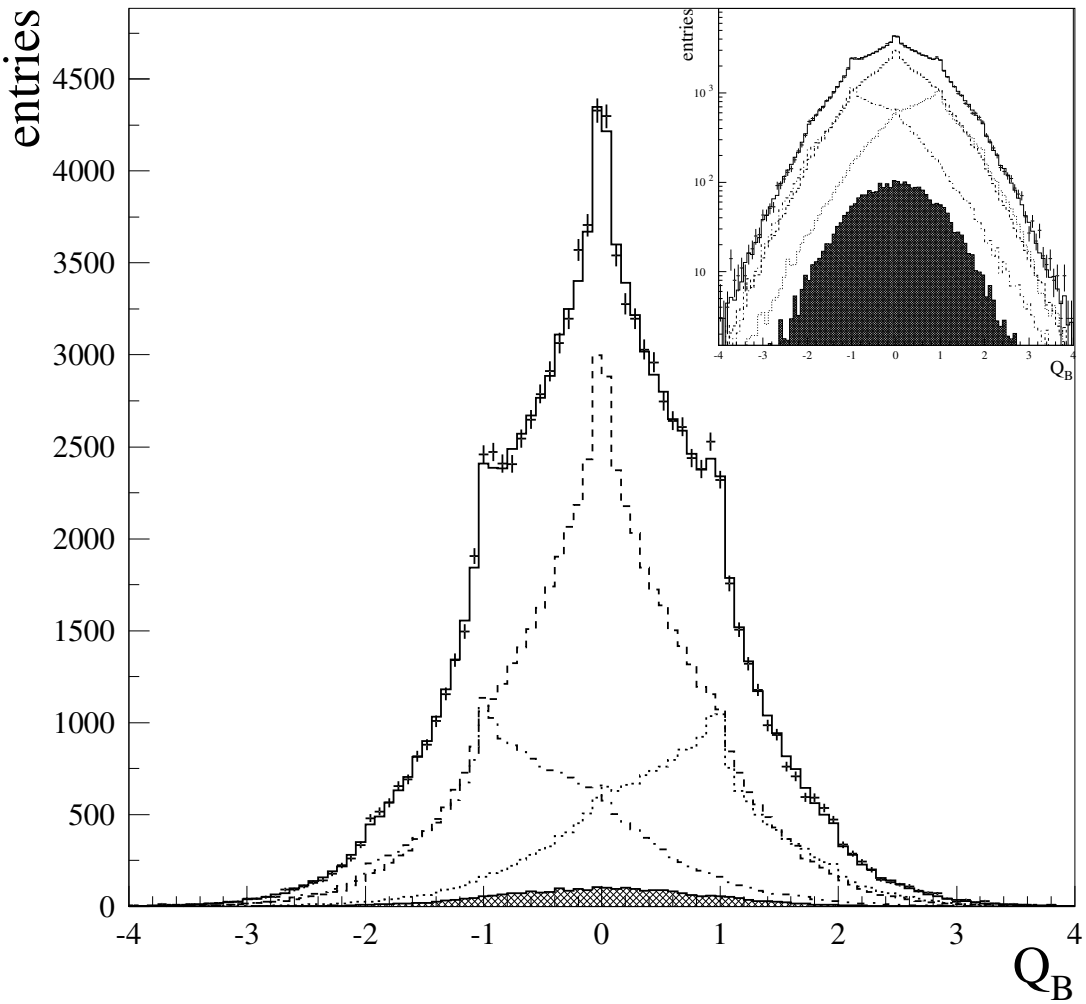

Figure 5: Distribution of the vertex charge, Q_B, of the weakly-decaying b-hadron for the data (points with error bars) with the result of the fit superimposed (solid histogram) on a linear scale and on a logarithmic scale (as inlay). The shapes for neutral (dashed histogram), negatively (dashed-dotted) and positively (dotted) charged b-hadrons obtained from the simulation (in the fit, one single component was used for positively and negatively charged b-hadrons) are also shown. The hatched histogram shows the contribution of non-$b\bar{b}$ events.

The measured Q_B distribution has been fit by the corresponding shapes expected for charged and neutral b-hadrons obtained from the simulation, while not separating the shapes for the positive and negative charges.

A technique based on a binned log-likelihood method taking into account the limited statistics of the simulation has been used [13]. The non-$b\overline{b}$ background has been fixed to the value obtained from simulation. The real data distribution, corresponding to 103.285 selected hemispheres, together with the fit result and the simulation prediction for neutral, positively and negatively charged b-hadrons is shown in Figure 5. The result for f^+, the fraction of charged b-hadrons in a sample of weakly-decaying b-hadrons produced in $Z^0 \to b\overline{b}$ decays, is $f^+ = (41.84 \pm 0.99(\text{stat.}))\%$ for the 1994 data set and $f^+ = (42.65 \pm 1.48(\text{stat.}))\%$ for 1995 giving a combined value of

$$f^+ = (42.09 \pm 0.82(\text{stat.}))\%. \tag{3}$$

The result for f^0 is given through $f^0 = 1 - f^+ = (57.91 \pm 0.82(\text{stat.}))\%$, with f^+ and f^0 being fully anticorrelated. The χ^2 per degree of freedom of the fits are 0.96 and 1.06 for the two years.

4 Systematic checks and uncertainties

Several cross-checks have been performed. The fit range and number of bins of the histograms used in the fit have been varied. The momentum cut has been varied in the range from 300 to 800 MeV/c and the maximum number of rejected tracks in the hemisphere between two and five. No significant change of the result has been found. The distributions of negatively and positively charged b-hadrons have been fit separately. This gives

$$\begin{aligned} BR(b,\overline{b} \to X_B^+) &= (20.66 \pm 0.60(\text{stat.}))\% \\ BR(b,\overline{b} \to X_B^-) &= (21.16 \pm 0.59(\text{stat.}))\%. \end{aligned}$$

for 1994 and

$$\begin{aligned} BR(b,\overline{b} \to X_B^+) &= (21.37 \pm 0.87(\text{stat.}))\% \\ BR(b,\overline{b} \to X_B^-) &= (21.29 \pm 0.86(\text{stat.}))\%. \end{aligned}$$

for 1995. The two numbers are correlated ($\rho^{\pm} \approx 0.44$).

As already mentioned and used for the calibration, the vertex charge Q_B can be used as flavour tag for hemispheres where the b- or $\overline{b}$-quark fragmented into a charged b-hadron and is thus sensitive to the forward-backward asymmetry A_b^{FB}. The differential asymmetry, computed from the vertex charges in the forward and backward hemispheres, versus the direction of the thrust axis is shown in Figure 6, showing good agreement with the expectation from the measured value of the pole asymmetry $A_b^{FB} = 0.0982 \pm 0.0017$ (from [1]).

To estimate systematic errors, the following parameters in the simulation and cuts have been varied:

- Lifetimes of b-hadrons.
- The oscillation frequency and thus the mixing probability χ_d for B^0-mesons. Mixing of B^0-mesons leaves the contribution from fragmentation particles unchanged but reverses the flavour of the weakly-decaying B-meson. The contributions to the vertex

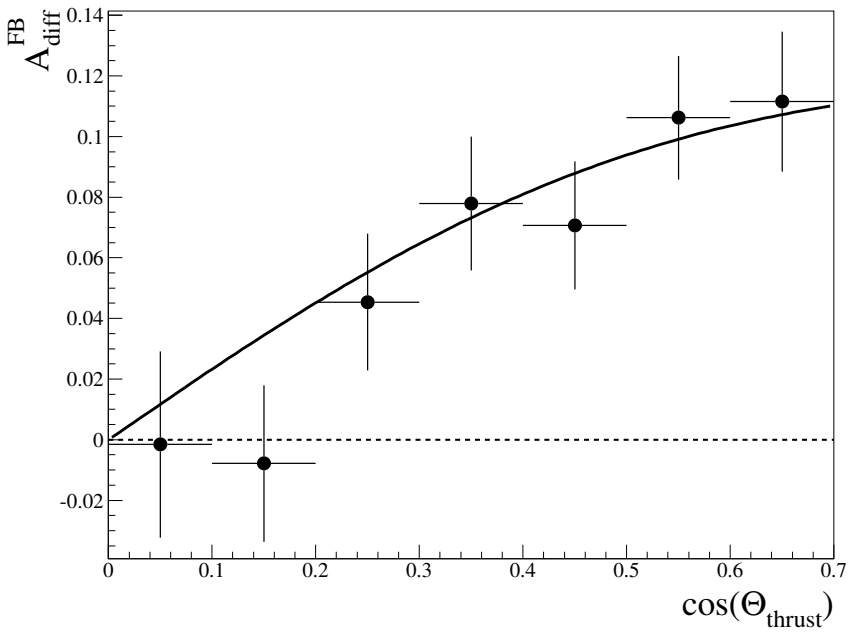

Figure 6: The dependence of the measured differential asymmetry A_{diff}^{FB} on $\cos\theta_{thrust}$ for the data. A_{diff}^{FB} has been computed from the vertex charges in the forward and backward hemispheres as: $A_{diff}^{FB} = (< Q_B^{FW} > - < Q_B^{BW} >)/ < Q_B^b >$, where $< Q_B^b >$ is the mean of the vertex charge for hemispheres containing a b-quark. The errors indicated are statistical only. The expectation for the pole asymmetry $A_b^{FB} = 0.0982$ (from [1]) is superimposed as solid line.

charge from B^0- and $\overline{B}^0$-mesons are slightly different. One reason is that B^0-mesons produce dominantly D^--mesons whereas $\overline{B}^0$-mesons mainly give D^+, leading to different charges at the tertiary charm vertex.

- The rates of different b-hadron species, because different b-hadrons contribute to a certain charge (e.g. B^0, B_s^0, Λ_b, Ξ_b^0 to $Q = 0$) and their distributions look slightly different. The value of $f_{B_u} (= f_{B_d})$ has been set to the measured value in this analysis. The values of f_{B_s} and $f_{b-baryon}$ from [1] have been rescaled accordingly to ensure $f_{B_s} + f_{b-baryon} + f_{B_u} + f_{B_d} = 1$.
- The rates of excited b-hadrons, namely orbitally excited $B_{u,d,s}^{**}$-mesons and $\Sigma_b^{(*)}$-baryons. The expected strong decays of these states produce particles (pions or kaons) looking partly like fragmentation particles (coming from the primary vertex) and partly like B-decay particles (having large rapidity). From the results in [14,15] an average $P_{B_{u,d}^{**}} = BR(\overline{b} \to B_{u,d}^{**})/BR(\overline{b} \to \overline{b}(u,d)) = 0.24 \pm 0.04$ is computed. It is assumed that $P_{B_s^{**}} = P_{B_{u,d}^{**}}$. For $\Sigma_b^{(*)}$ production DELPHI gives an upper limit in [15]. The following value is taken as a conservative choice[6]: $P_{\Sigma_b^{(*)}} = 0.10 \pm 0.05$.
- The rate of so called 'wrong-sign charm' production at the upper W vertex from [16].
- The branching ratios of 'right-sign' decays of B^+- and B^0-mesons into $\overline{D}^0$- and D^--mesons. Because of $\tau(D^-) > \tau(\overline{D}^0)$, b-hadron decays with a D^- in the final state have charged particles from the tertiary charm decay which are more displaced from the primary vertex than in the case of a $\overline{D}^0$, affecting the vertex variables

[6] $P_{\Sigma_b^{(*)}}$ is defined in the same way as $P_{B^{**}}$.

source	value and variation	$\delta f^+[\%]$
τ_{B^0}	(1.542 ± 0.016) ps	$+0.007$
τ_{B^+}	(1.674 ± 0.018) ps	-0.129
τ_{B_s}	(1.461 ± 0.057) ps	$+0.027$
$\tau_{b-baryon}$	(1.208 ± 0.051) ps	$+0.010$
χ_d	0.181 ± 0.004	$+0.038$
f_{B_s}	(8.5 ± 1.3) %	$+0.217$
$f_{b-baryon}$	(9.5 ± 2.0) %	$+0.057$
$f_{\Xi_b^-}$	(1.1 ± 0.5) %	-0.187
$P_{B^{**}}$	0.24 ± 0.04	$+0.287$
$P_{\Sigma_B^{(*)}}$	0.10 ± 0.05	-0.027
wrong sign charm rate	(20.0 ± 3.3) %	-0.001
$BR(B^{0(+)} \to \overline{D}^{-(0)} + X)$	text	-0.183
b fragmentation function	text	0.201
min. # of acc. charged particles	4,3	0.217
Q_B calibration	text	0.677
non-$b\overline{b}$ background	$\pm 30\%$	$+0.113$
total		0.886

Table 1: Breakdown of systematic errors on f^+. For the b-hadron fractions, f_{B_s} and $f_{b-baryon}$, their correlation has been taken into account, for the other sources of systematic uncertainties the errors have been added in quadrature. The signs of the errors given are for an upwards variation of the corresponding physics parameter. For $BR(B^{0(+)} \to \overline{D}^{-(0)} + X)$, an upwards variation means increasing $BR(B^0 \to D^- + X)$ and adjusting the other, related branching ratios as explained in the text.

used as input to the neural network. The following branching ratios have been used, being consistent with the measured inclusive production rates of $\overline{D}^0$- and D^--mesons in B-decays: $BR(B^0 \to D^- + X) = 15.6\%$, $BR(B^0 \to \overline{D}^0 + X) = 65.8\%$, $BR(B^+ \to D^- + X) = 29.3\%$, $BR(B^+ \to \overline{D}^0 + X) = 52.1\%$. These branching ratios have been varied by 5% (absolute). The variation has been performed in a correlated way to keep the total rate of $\overline{D}^0$- and D^--mesons in B-decays and $BR(B^0/B^+ \to \overline{D}^0 + X) + BR(B^0/B^+ \to D^- + X)$ constant.

- The b-quark fragmentation function. The measured function from DELPHI [17] has been used. For the systematic error the full difference to the model implemented in the simulation (Peterson with $\epsilon_b = 0.002326$) has been taken. This is a conservative choice, since the measurement errors are much smaller than the deviations from the fragmentation function in the simulation.
- The cut on the minimum number of accepted charged particles in the hemisphere used for the calculation of Q_B has been changed from an even to an odd number. This could have a systematic effect because charged (neutral) b-hadrons decay to an odd (even) number of charged particles.
- The calibration of the vertex charge (described in Section 3). The parameters a_1 and a_2 have been varied independently in a way which results in a displacement of the f^{OS} versus Q_B^{cut} curve (Figure 4) in the simulation, corresponding to a shift by one standard deviation with respect to the data errors. This procedure has been

consistently applied also to the 1995 year simulation, even if no correction has been applied in this case, because of the good agreement between data and simulation. The error from the parameter giving the largest variation in f^+ has been chosen.
- The non-$b\overline{b}$ background (mainly $c\overline{c}$) has been varied by $\pm 30\%$.

If not explicitly stated otherwise, the corresponding numbers have been taken from [1]. The breakdown of the systematic errors is shown in Table 1. The result, including systematic errors, is:

$$f^+ = (42.09 \pm 0.82(\text{stat.}) \pm 0.89(\text{syst.}))\%. \tag{4}$$

5 Interpretation of the results

Weakly-decaying neutral b-hadrons are B^0- and B_s^0-mesons, the Λ_b-baryon and the strange b-baryon Ξ_b^0. The rate of charged b-hadrons is dominated by the B^+-meson, strange b-baryons giving only a minor contribution (Ξ_b^-, Ω_b^-). Formally, one gets:

$$\begin{aligned} f^0 &= f_{B_d} + f_{B_s} + f^0_{b-baryon}, \\ f^+ &= f_{B_u} + f^+_{b-baryon}. \end{aligned} \tag{5}$$

In [16], the fraction of Ξ_b^--baryons has been estimated analysing production rates of $\Xi^- l^-$ final states: $f_{\Xi_b^-} = BR(\overline{b} \to \overline{\Xi}_b^+) = BR(b \to \Xi_b^-) = (1.1 \pm 0.5)\%$. This fraction is subtracted from f^+ to get the fraction of B^+-mesons in a sample of weakly-decaying b-hadrons produced in the fragmentation of $\overline{b}$-quarks (the production fraction of Ω_b^--baryons is expected to be negligible). The result is

$$f_{B_u} = (40.99 \pm 0.82(\text{stat.}) \pm 1.11(\text{syst.}))\%, \tag{6}$$

where the error from $f_{\Xi_b^-}$ has been added to the systematic error from f^+ taking into account the correlation arising from the fact that the uncertainty of $f_{\Xi_b^-}$ is a source of uncertainty for f^+ (compare Table 1).

6 Conclusions

A precise measurement of the production fractions of weakly-decaying charged and neutral b-hadrons has been presented for the first time. The fraction of $\overline{b}$-quarks fragmenting into positively charged weakly-decaying b-hadrons, and thus the fraction of charged b-hadrons in a sample of weakly-decaying b-hadrons produced in $Z^0 \to b\overline{b}$ decays, has been measured to be $f^+ = (42.09 \pm 0.82(\text{stat.}) \pm 0.89(\text{syst.}))\% = (42.09 \pm 1.21)\%$. Subtracting the $\overline{\Xi}_b^+$ rate (assuming that the $\overline{\Omega}_b^+$ rate is negligible) gives $f_{B_u} = (40.99 \pm 0.82(\text{stat.}) \pm 1.11(\text{syst.}))\% = (40.99 \pm 1.38)\%$. This is, so far, the most precise dedicated measurement of a production fraction of a specific b-hadron. The accuracy on f_{B_u} is comparable to the accuracy achieved by combining all other information available on b-hadron production fractions. This measurement thus represents significant new information that will impact on combinations of measurements to estimate b-hadron production fractions in jets.

Acknowledgements

We are greatly indebted to our technical collaborators, to the members of the CERN-SL Division for the excellent performance of the LEP collider, and to the funding agencies

for their support in building and operating the DELPHI detector.
We acknowledge in particular the support of
Austrian Federal Ministry of Education, Science and Culture, GZ 616.364/2-III/2a/98,
FNRS–FWO, Flanders Institute to encourage scientific and technological research in the industry (IWT), Federal Office for Scientific, Technical and Cultural affairs (OSTC), Belgium,
FINEP, CNPq, CAPES, FUJB and FAPERJ, Brazil,
Czech Ministry of Industry and Trade, GA CR 202/99/1362,
Commission of the European Communities (DG XII),
Direction des Sciences de la Matière, CEA, France,
Bundesministerium für Bildung, Wissenschaft, Forschung und Technologie, Germany,
General Secretariat for Research and Technology, Greece,
National Science Foundation (NWO) and Foundation for Research on Matter (FOM), The Netherlands,
Norwegian Research Council,
State Committee for Scientific Research, Poland, SPUB-M/CERN/PO3/DZ296/2000, SPUB-M/CERN/PO3/DZ297/2000 and 2P03B 104 19 and 2P03B 69 23(2002-2004)
JNICT–Junta Nacional de Investigação Científica e Tecnológica, Portugal,
Vedecka grantova agentura MS SR, Slovakia, Nr. 95/5195/134,
Ministry of Science and Technology of the Republic of Slovenia,
CICYT, Spain, AEN99-0950 and AEN99-0761,
The Swedish Natural Science Research Council,
Particle Physics and Astronomy Research Council, UK,
Department of Energy, USA, DE-FG02-01ER41155,
EEC RTN contract HPRN-CT-00292-2002.

References

[1] Particle Data Group, K. Hagiwara et al.; *Phys. Rev.* **D66** (2002) 010001.

[2] DELPHI Collaboration, P. Abreu et al.; *Phys. Lett.* **B289** (1992) 199;
OPAL Collaboration, P.D. Acton et al.; *Phys. Lett.* **B295** (1992) 357;
ALEPH Collaboration, D. Buskulic et al.; *Phys. Lett.* **B361** (1995) 221.

[3] CDF Collaboration, T. Affolder et al.; *Phys. Rev. Lett.* **84** (2000) 1663;
CDF Collaboration, F. Abe et al.; *Phys. Rev.* **D60** (1999) 092005.

[4] DELPHI Collaboration, P. Abreu et al.; *Z. Phys.* **C68** (1995) 375;
DELPHI Collaboration, P. Abreu et al.; *Z. Phys.* **C68** (1995) 541;
ALEPH Collaboration, D. Buskulic et al.; *Phys. Lett.* **B384** (1996) 449;
ALEPH Collaboration, R. Barate et al.; *Eur. Phys. J.* **C2** (1998) 197.

[5] ALEPH Collaboration, R. Barate et al.; *Eur. Phys. J.* **C5** (1998) 205.

[6] T. Sjöstrand, *Comp. Phys. Comm.* **82** (1994) 74;
T. Sjöstrand, CERN-TH.7112/93.

[7] DELPHI Collaboration, P. Abreu et al.; *Z. Phys.* **C73** (1996) 11.

[8] DELSIM User's Guide, DELPHI Note 89-15 PROG 130;
DELSIM Reference Manual, DELPHI Note 89-68 PROG 143.

[9] DELPHI Collaboration, P. Aarnio et al.; *Nucl. Instrum. Methods* **A303** (1991) 233.

[10] DELPHI Collaboration, P. Abreu et al.; *Nucl. Instrum. Methods* **A378** (1996) 57.

[11] DELPHI Collaboration, J. Abdallah et al.; CERN-EP/2002-088 (submitted to *Eur. Phys. J.* **C**)

[12] DELPHI Collaboration, P. Abreu et al.; *Phys. Lett.* **B475** (2000) 429;
DELPHI Collaboration, P. Abreu et al.; *Eur. Phys. J.* **C20** (2001) 617.

[13] R. Barlow, C. Beeston, *Comp. Phys. Comm.* **77** (1993) 219.

[14] OPAL Collaboration, R. Akers et al.; *Z. Phys.* **C66** (1995) 19;
DELPHI Collaboration, P. Abreu et al.; *Phys. Lett.* **B345** (1995) 598;
ALEPH Collaboration, D. Buskulic et al.; *Z. Phys.* **C69** (1996) 393;
ALEPH Collaboration, R. Barate et al.; *Phys. Lett.* **B425** (1998) 215;
L3 Collaboration, M. Acciarri et al.; *Phys. Lett.* **B465** (1999) 323;
CDF Collaboration, T. Affolder et al.; *Phys. Rev.* **D64** (2001) 072002.

[15] C. Weiser, Proceedings of the 31st International Conference on High Energy Physics, ICHEP 2002, Amsterdam, 2002, pp. 607-609; *S. Bentvelsen, P. de Jong, J. Koch and E. Laenen (Editors)*, Elsevier Science BV

[16] ALEPH, CDF, DELPHI, L3, OPAL, SLD; CERN-EP/2001-050.

[17] K. Harder, Proceedings of the 31st International Conference on High Energy Physics, ICHEP 2002, Amsterdam, 2002, pp. 535-538; *S. Bentvelsen, P. de Jong, J. Koch and E. Laenen (Editors)*, Elsevier Science BV